ABSTRACT

This study investigates the use of RAPRENO$_X$, a non-catalytic selective reduction technology, to reduce nitrogen oxides in exhaust from a 150kW gas turbine exhaust. An exhaust system was designed and constructed in order to test the effects of load (temperature), exhaust composition, and means of cyanuric acid injection on the process. The major accomplishments of this project was the successful demonstration of the process and improved understanding on system. With a simple cyanuric acid/water slurry injection system, 18 ppm NO_x was obtained in the gas turbine exhaust. In addition an extended model was developed to explore the effects of recirculation and fuel injection on NO_x reduction.

TABLE OF CONTENTS

LIST OF FIGURES

List of Tables

1.0 BACKGROUND

With the major emphasis on meeting the goal of the 1990 Federal Clean Air Act, strict restrictions on new sources of nitrogen oxide emissions will be enforced in those areas that presently do not meet federal standards for air quality. These restrictions may impact on our nation's ability to drill for oil on offshore oil platforms where environmental concerns have already made oil exploration more difficult. The use of gas turbines on off-shore oil platforms accounts for approximately 65% of the NO_X emitted during oil exploration. Thus, a safe, cost-effective, reliable NO_X control technology for gas turbines is needed to aid in minimizing the impact of pollution control on our ability to drill for oil.

RAPRENOx, a patented process currently being commercialized in diesel engines, promises to be suitable for this type of application. The process uses isocyanic acid, formed by the thermal decomposition of cyanuric acid, a non-toxic, nonflammable, commercially available solid material. The gaseous isocyanic acid, derived from cyanuric acid added to the exhaust stream reduces NO_X to N_2, N_2O, H_2O and CO_2. The fact that cyanuric acid is a solid nontoxic compound, in contrast to ammonia, makes it well suited to off-shore applications.

Another significant difference to most other post combustion selective NO_X abatement schemes that use ammonia or urea is that temperature boost and NO_X reduction are achieved simultaneously. The added fuel enhances the initiation of the NO_X reduction mechanisms by increasing the radical pool and thereby lowering the temperature requirement and the associated energy input. Recirculation decreases residence time and reactor size. Mixing of reagent and fuel occur in parallel, making elaborate injection schemes superfluous. The lean premixed combustion of the added fuel produces a negligible contribution to the overall NO_X content.

2.0 TECHNICAL APPROACH:

A research program consisting of a combination of experimental and modeling efforts was conducted to further characterize, develop, and assess the RAPRENO$_X$ process for NO_X control in gas turbines. The major goal of this research was to develop the necessary skills for reactor and delivery systems design to scale the approach to larger gas turbines. As part of this research effort a number of tasks were undertaken to reach the objective of our first demonstration of NO_X in a gas turbine. It was necessary to purchase and install a used gas turbine (model Garrett GTP 70-52) and incorporate a water break to load the unit. A major effort was undertaken to build and test an effective reactor that incorporates a recirculation zone to stabilize the lean burning mixture. In addition, an effective reactant injection scheme was developed to reliably supply cyanuric acid in a controlled manner. Finally, a data acquisition

system was installed and integrated into the design to allow for automated data acquisition. Besides the experimental approach, a modeling effort was undertaken to incorporate mixing with chemistry to predict effects of reactor design on optimum performance.

2.1 Experimental Setup

All experiments were performed in the Combustion Laboratories at the University of California in Berkeley, California. The laboratory has been partitioned and insulated to reduce emitted noise from the gas turbine. The building is equipped with an exhaust stack and the test cell, the partitioned section of the laboratory, has a separate fan driven air supply and exhaust vent. A double window allows visual access to the test stand and the turbine and reactor room experiments were controlled from outside of the laboratory. The experimental setup consists of two independent units, a 150 kW rated stationary gas turbine with the sole purpose of producing exhaust gases, and an exhaust gas treatment reactor (Figure 1). The turbine used in this investigation produces relatively low NO_x emissions of 30 to 40 ppm at full load. That has the advantage that with additional NO doping exhaust gas compositions of much larger, more efficient turbines can be simulated. To produce homogeneous NO_x distribution in the exhaust gases pure NO is introduced through a mass flow controller into the turbine intake air stream, resulting in steady NO_x emissions at any desired level. Exhaust gas analysis concluded that most of the added NO survives as it passes through the combustion chamber of the turbine. In this study, concentrations of NO_x at 100 to 200 ppm were generated to match most commonly used older gas turbines.

Both process reagent and the additional fuel are injected directly into the exhaust gas stream as it leaves the turbine and mixed in the highly turbulent flow through a 12 inch diameter pipe connecting the engine to the reactor. The treated flue gases exit the system, are cooled by water injection and vent through a fan-assisted stack.

2.1.1 Gas Turbine and Dynamometer

The used turbine engine is a Garrett GTP 70-52 industrial style gas turbine with a rated maximum output of 150 kW. It has a dual stage centrifugal compressor and a single turbine wheel. Compressor and turbine wheels are mounted on the same primary shaft. Its speed is governed mechanically to 40800 rpm (680 s^{-1}). A planetary transmission reduces output shaft speed to 6000 rpm (100 s^{-1}). A dynamically balanced connecting shaft specifically designed for this application links the engine output to a Stuska S 400 water brake dynamometer, which provides controllable load up to 300 kW.

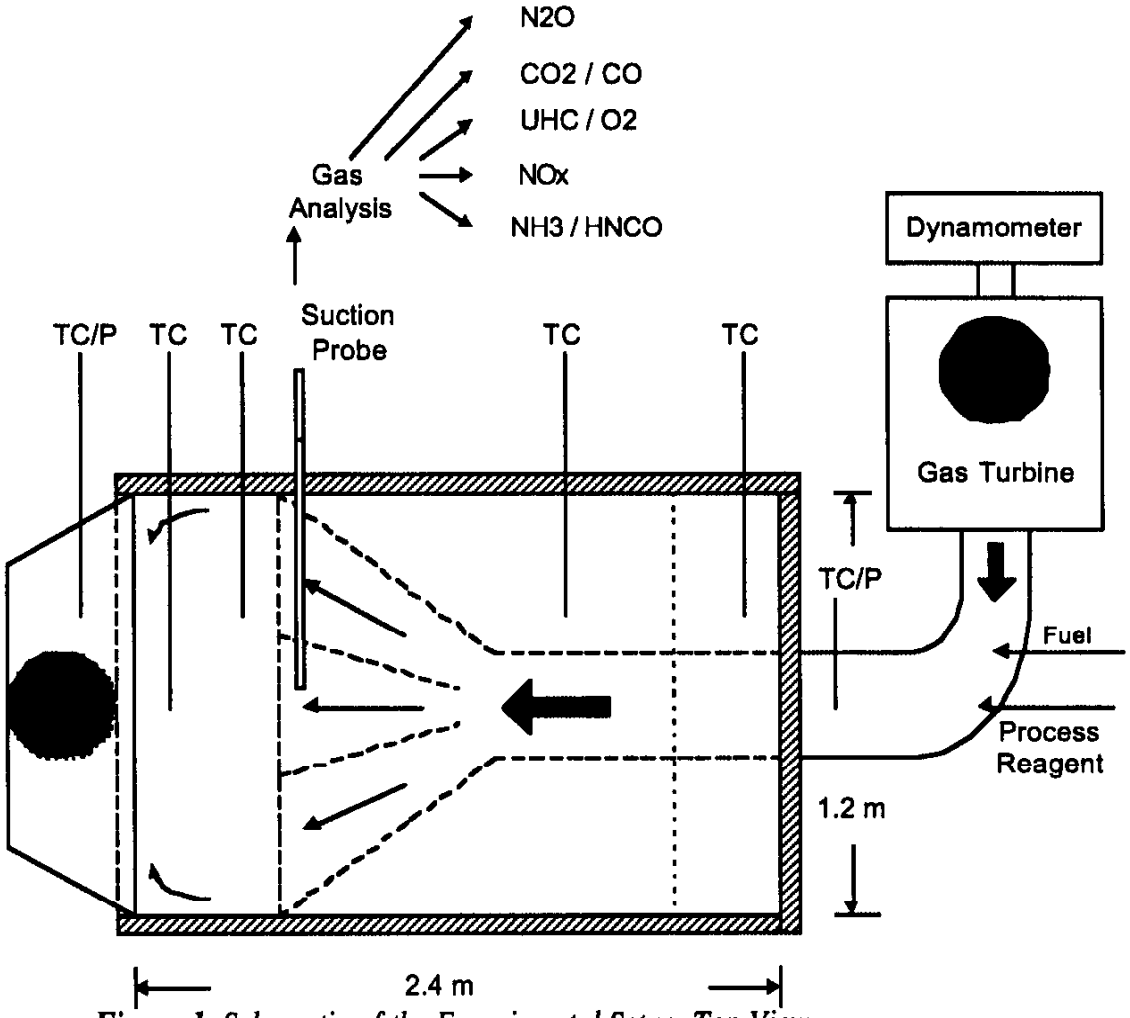

Figure 1. Schematic of the Experimental Setup, Top View.

Engine and dynamometer are both aligned and rigidly mounted to the laboratory floor. The water brake dynamometer transforms mechanical energy into heat via viscous dissipation. The water level in the sealed dynamometer chamber is directly related to the braking power applied on the turbine. The amount of the so applied load is controlled by regulation of the input water flow. This is done remotely with a step motor powered gear reduction drive attached to a water control valve. A torque arm is linked to a pressure transducer, which keeps the otherwise freely rotating dynamometer chamber stationary. Using transducer pressure, torque arm length and rotational speed allows computation of the dissipated power. This dynamometer has, in contrast to an eddy current dynamometer, very low inertia. Low initial load and inertia allows rapid acceleration of the turbine during startup. The high acceleration is necessary since starting cycles are timed. A shut down is automatically triggered when steady state speed is not reached within 30 seconds. Load

following and speed control are achieved in the turbine engine by varying fuel injection pressure and corresponding fuel input.

A gas turbine is a heat engine and is therefore dependent on the temperature and pressure of its working fluid. Input air quality has an immediate affect on the cycle efficiency. To improve efficiency, minimize transients, and to assure stable steady state operation, cool filtered air is supplied directly to the unit with a fan from the outside of the building. Intake temperature is continuously monitored. The air flows into the centrifugal compressor, which boosts the pressure in the plenum chamber to 35 psi (i.e. it reaches a pressure ratio, p = 2.4). Diesel fuel is injected into a reverse flow can combustor mounted on the plenum to interact with the compressed intake air. The so obtained fuel – air stream is then ignited and combusts, resulting in a stable non-premixed overall lean burning combustion process.

Following combustion these hot compressed gases enter the turbine nozzle and expand through the turbine wheel where power is extracted to drive compressor, engine accessories and provide output shaft power. Under laboratory conditions steady state maximum load was determined to be approximately 90 kW, with a thermal input of ~800 kW.

2.1.2 Post Turbine Auxiliary Fuel Injection

To allow operation at a fixed reactor temperature, the amount of fuel added to the exhaust gas stream has to be controlled. To this end, a controllable pump provides water-cooled Diesel to a calibrated stainless steel injector nozzle mounted in the center of the exhaust duct between turbine and reaction chamber. A control unit, receiving its signal from a PID controller coupled to the reactor temperature drives the pump. It delivers 100 ml/min to 450 ml/min of Diesel fuel, depending on exhaust gas temperature and target operating conditions. Fuel flow is monitored with a Matheson 604 rotameter. A solenoid valve provides emergency shut off. The injection nozzle is pointed into the direction of flow and produces an 90 degree cone when fluid is expelled into a still body of air.

2.1.3 Cyanuric Acid Injection

Mixing of exhaust gases with the proper amount of CYA is crucial to the NO removal efficiency. It is therefore important to be able to continuously meter and control the quantity of CYA that is injected. In these experiments, CYA is injected as a water slurry. Using an incompressible fluid, such as facilitates reliable CYA injection over a wide range of feed rates. Automated control mechanisms are employed to allow load following and NO_x content based variation of these injection rates. In order to benefit from turbulent mixing CYA is introduced as far upstream from the reactor as possible.

Prior to the gas phase NO reduction the injected reagent has to sublime and decompose from CYA, $(HNCO)_3$, to isocyanic acid (HNCO). This occurs at temperatures above 330°C. Any injection system therefore has to be able to

withstand exhaust gas temperatures and to deliver a spray of particles that are small enough to sublime in the hot coflow before entering the reaction zone. Since earlier efforts have shown that dry powder injection is troubled with injector clogging and does not appear to be practical in an industrial application, a different mode of injection, using water as a carrier, has been chosen.

When cyanuric acid is mixed with water, a slurry is formed. To insure a homogeneous distribution of the suspended particles in the water, this suspension has to be continuously agitated. This is done by a pump circulating the mixture, at a rate of approximately 50 l/min, from the bottom to the top of a 25-liter storage container. (See Figure 2.)

A Bailey SLC 1 controller operates a peristaltic pump to deliver the desired amount of slurry through a 4 mm inner diameter tube from the holding container to the injector. NO_x concentration and reagent/water ratio are manually input into the controller. Tubing, carrying the slurry to the injector, is sized such that the flow velocity prohibits settling out of the reagent powder.

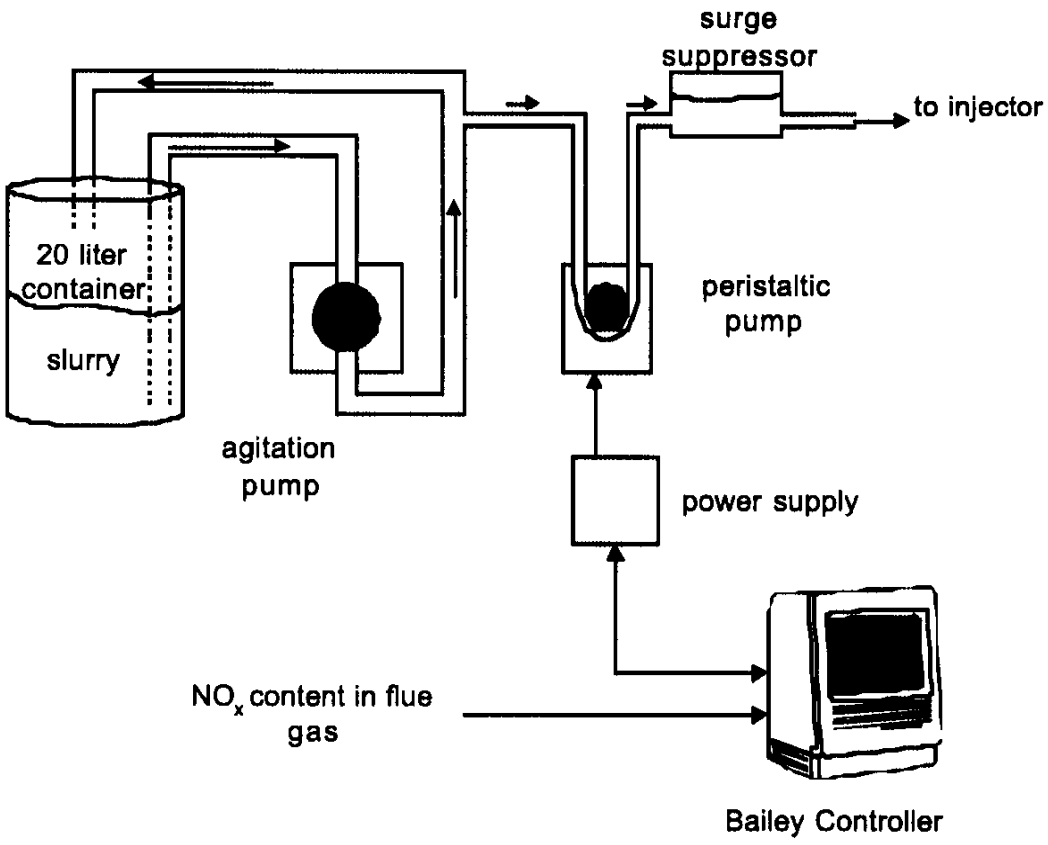

Figure 2. Schematic of the Slurry Supply System

Two different injection systems have been built: a motor driven rotary style, water-cooled injector and a compressed air assisted coaxial injector. (See Figure 3. and Figure 4.) Both allow injection of various amounts of slurry of different consistency into the hot turbine exhaust stream. Droplet size was found to be a dependent on rotational speed or compressed air flow respectively. Pressure drops across the injectors were negligible in both cases at given slurry flow rates. Injection occurs parallel to the flue gas flow 70 - 90 cm upstream of the reaction chamber. The injector is fitted through an access port in the duct and can be inserted to various depths, thereby changing the injection location.

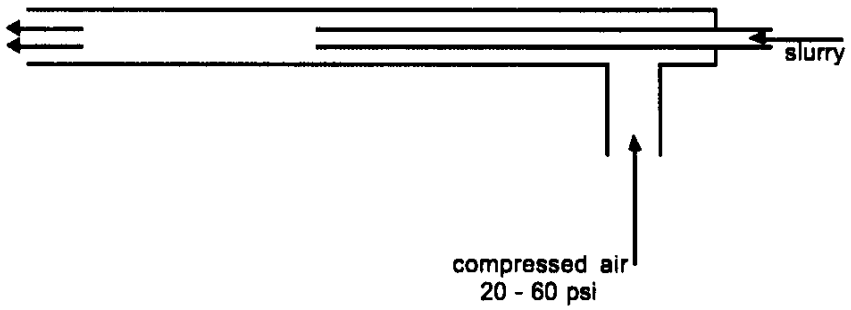

Figure 3. Schematic of Air Assisted Injector

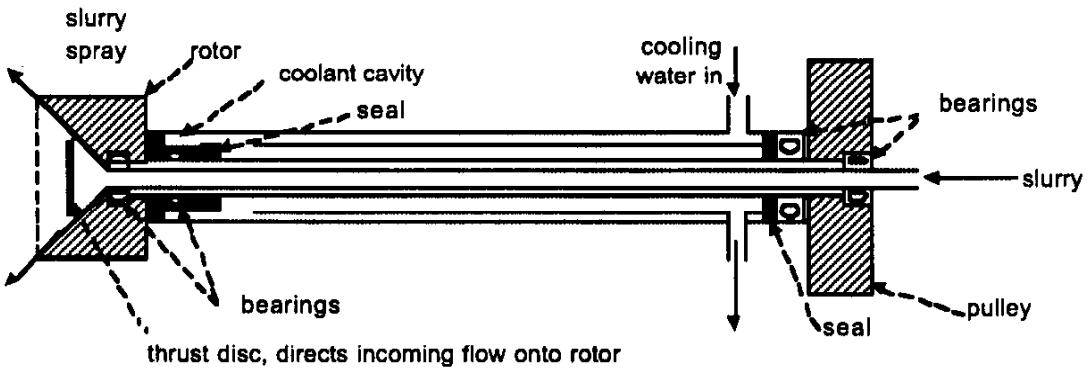

Figure 4. Schematic of Motor Driven Rotary Injector

2.1.4 Reaction Chamber

In the design of the reaction chamber the following constraints were considered:

1) The reaction chamber has to be large enough to allow sufficient residence time for autoignition of the added fuel and NO removal;
2) Reactor geometry has to induce recirculation of the incoming flow;
3) The exhaust gases have to be guided through the reactor without significant pressure loss;
4) The entire reactor system has to fit into the laboratory, the turbine and reactor overall dimensions must be manageable.

These requirements are best met with a rectangular design. Steel angles provide structural strength to the bolted shell and support its 16 gauge sheet metal walls. The reactor is internally insulated with 3.5 in (~ 8.89 cm) rigid insulation. The insulation can withstand 2000 K with a total thermal conductivity rating of k = 1.11 W/K-m^2. The overall volume of the reactor is 5.44 cubic meter, which translates to a maximum residence time of about 2 seconds at a temperature of 750ºC. The recirculation zone is approximately 2.5 cubic meters.

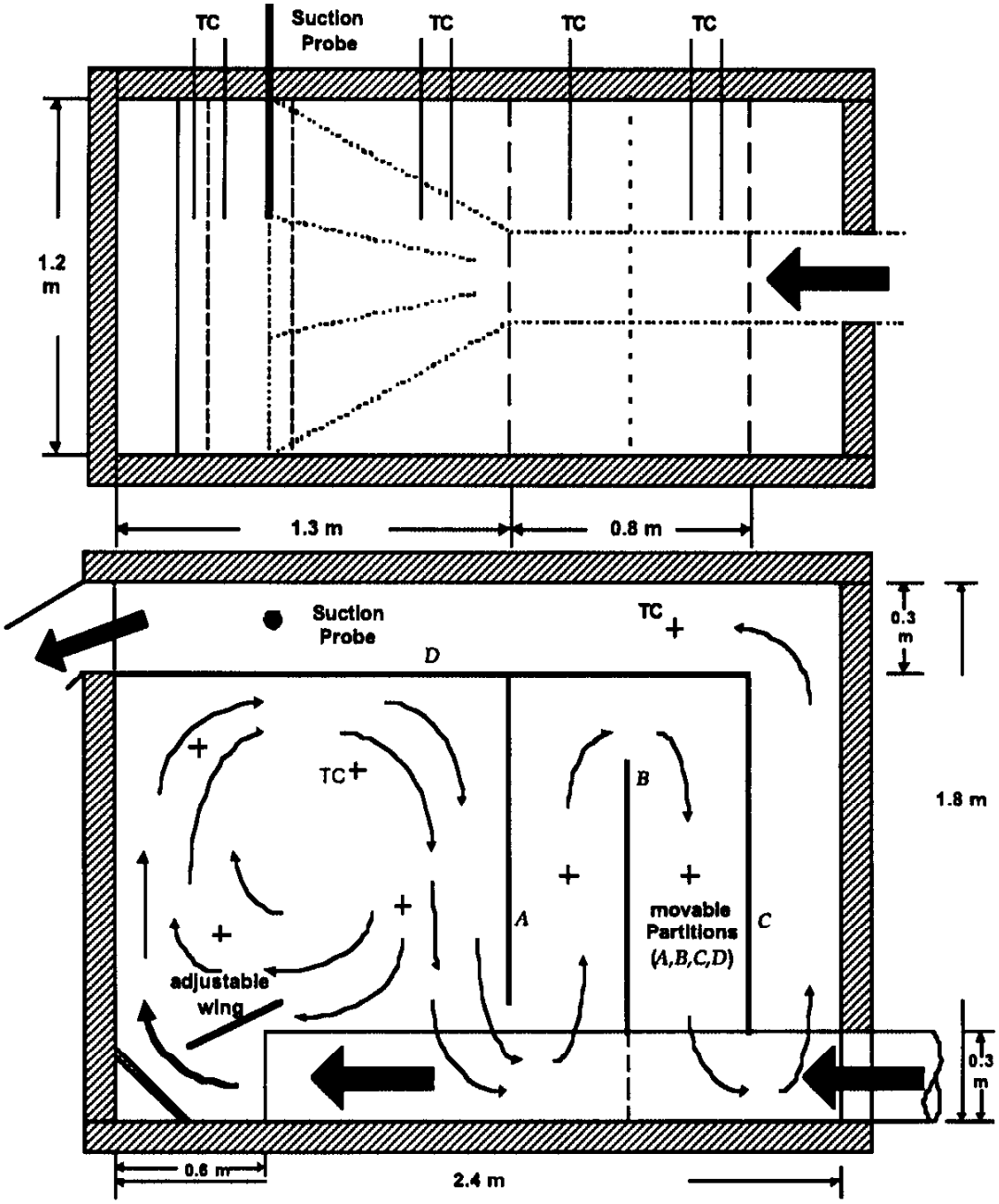

Figure 5. Schematic of the Reaction Chamber

All surfaces have been coated with a ceramic insulation rigidizer and sealant to minimize erosion and catalytic interactions. The chamber is partitioned with ceramic rigid insulation boards supported on stainless steel angles. Two doors facilitate access to the chamber. Moving of the partitions can vary flow geometry as well as the primary chamber size. The reaction chamber as a whole remains

unchanged. See Figure 6 for a schematic of the reactor. Thermocouples, pressure tabs as well as a water-cooled suction probe are inserted through the insulated walls.

2.2 Exhaust Gas Analysis

Exhaust gases are sampled continuously. A water cooled suction probe is located downstream of the reaction chamber. A sample pump, with attached filter, provides 5 psi of exhaust sample pressure to an analysis station. Suction probe, pump, filter and connecting teflon line are heated above the dew point of water (~ 70°C). A gas phase "Nafion" membrane sample dryer removes selectively water vapor so that all measurements are taken on a dry gas basis. Gas composition analysis is performed by a set of Horiba instruments consisting of:

A **CLA – 220 Chemiluminescent NO/ NO_x** analyzer.
An **AIA – 210 / 220 Infrared CO / CO_2** analyzer.
An **FIA – 220 Flame Ionization HC** analyzer.
An **MPA – 220 Magneto Pneumatic O_2** analyzer.

The analyzers are calibrated directly before experiments using certified calibration gases with concentrations of approximately 80 – 90% of the working range. Measurements of other relevant exhaust gas components not listed above such as reagent slip and N_2O are performed separately.

2.2.1 Determination of NH_3 and HNCO in Exhaust Gases

There are various techniques available to perform an NH_3 or HNCO analysis.[1] Using the instrumentation available at UCB, a wet chemical approach was chosen that used an NH_3 electrode.

To determine the concentration of both substances in the same sample, exhaust gases are passed through a series of wash bottles containing a basic 0.1M NaOH solution. The throughput is monitored with a rotameter and stopwatch. With the measured sample temperature at that point, the sample mass flow can be computed.

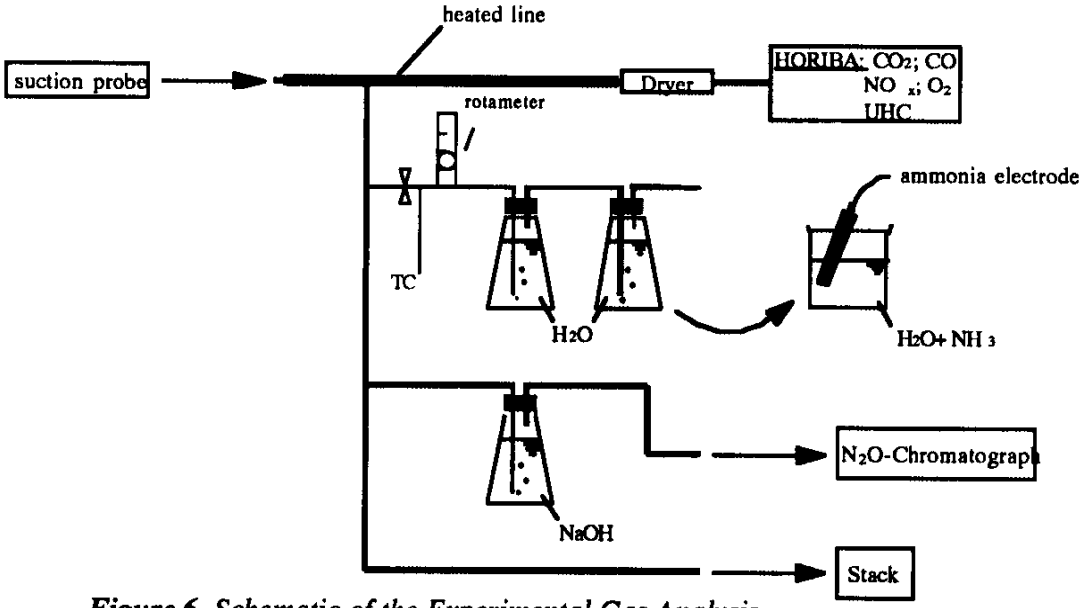

Figure 6. Schematic of the Experimental Gas Analysis

By using two wash bottles in series and combining the solutions, 99% absorption can be obtained. The quality of absorption can be quantified by analyzing each of the bottle's contents separately. The larger the ratio of the amount of ammonia detected in the first to that detected in the second the higher the absorption. In the experiment more than 95% absorption has been determined.

Once the NH_3 concentration, from the combined content of both containers, has been established, a strong acid, either HCl or H_2SO_4 solution (0.1M) is added to the sample solution. This lowers the pH sufficiently (a pH of < 5 is suggested by Elsener) to initiate hydrolyzation of HNCO according to:

$$HNCO + H_2O = NH_3 + CO_2$$

A repeated NH_3 determination will now also include the concentration of NH_3 from any HNCO slip. The difference in both measurements is the concentration of HNCO in the sample solution. Knowing the volume of the sample solution, the degree of absorption and the mass flow of the exhaust gas that passed through the sample solution allows the calculation of the concentration of NH_3 and HNCO in the exhaust gas stream. With the given electrode sensitivity a minimum concentration of 5 ppm of HNCO in the flue gas stream can be detected with 10 liters of gas sampled. For a schematic of the gas analysis see Figure 6.

2.2.2 Determination of N_2O in Exhaust Gases

The determination of N_2O in this study was performed using an SRI gas chromatograph with an electron capture detector (ECD). Samples were drawn through a NaOH solution to scrub out any SO_x in the exhaust gas stream. Samples were taken in Tedlar bags to the gas chromatograph. These bags had been flushed with nitrogen and evacuated prior to the experiments. The gas chromatograph was operated at a temperature of 50°C with a mixture of argon and methane as carrier gas. A Porapak Q separation column and a Porapak N back flush column were used. The ECD oven was heated to 349°C.

2.3 Data Acquisition

With the exception of HNCO and N_2O concentration measurements, all temperature, pressure and gas composition data were collected at a 1Hz frequency. Adam modules processed the incoming data remotely. The modules communicated with a PC through an RS 232 serial port. All information was displayed on screen and written to file during the experiments.

3.0 EXPERIMENTAL RESULTS

3.1 Gas Turbine Operating Conditions

The turbine was found to start and run reliably with the attached dynamometer and described exhaust duct. The backpressure of reactor and exhaust stack combined reached a maximum of 10 cm of H_2O at maximum reactor temperature. Peak dynamometer loads up to 105 kW were achieved, but could not be sustained at air intake temperatures above 19°C. In order to have repeatable test conditions the turbine was operated at a constant 90 kW dynamometer setting, which will be referred to as 100% load. At a lower heating value of 41.5 MJ/kg Diesel fuel the total energy input ranged between 760 and 860 kW. Intake temperatures were recorded between 17 and 32°C, depending on weather conditions. Exhaust gas temperatures were found to remain mostly in a range of 600 to 630°C. Average steady state conditions are summarized as follows in Table I.

Turbine Engine:	
Load	90 kW +/- 1 kW
Intake temperature	18 – 32°C
Exhaust temperature	600 – 630°C
Fuel consumption	1.11 – 1.25 kg/min
Air flow rate	0.97 – 1.08 kg/sec (constant)

Exhaust Gas Composition:	
O_2	14.5 – 15.1 %
CO_2	3.7 – 4.1 %
CO	280 – 390 ppm
NO_x	18.5 – 23.5 ppm (@15%O_2, dry)
HC	60 – 70 ppm

Table I. Average Experimental Steady State Turbine Operation Conditions

3.2 Reactor Operating Conditions

The average recirculation reactor temperature was controlled at a range of 700 to 800°C, with a mean residence time inside the recirculation zone of 710 to 650 msec respectively. Since turbine exhaust has a temperature between 600 and 650°C at full turbine load, the gas temperature had to be increased by 50 to 150°C. This desired temperature rise in the reactor was obtained via autoignition of auxiliary Diesel fuel, injected into the hot turbine exhaust duct between turbine and reactor. The auxiliary fuel needed to increase the reactor temperature to 700 – 800°C was 14 – 30% of the turbine fuel consumption. Figure 7 shows the measured amount of auxiliary fuel input for specific temperature rises. At full load and maximum auxiliary fuel injection, steady state conditions were reached within minutes. With the decay of thermal transients, auxiliary fuel flow was decreased to a constant, corresponding to the desired reactor temperature.

The reactor geometry (see Figure 3) allowed for 30 to 40% recirculation, a value determined with the water model. The steady state pressure drop across the reactor was found to be 65 mm water at constant steady state intake air mass flow (~ 1 kg/s). Reactor chamber insulation reduced average reactor outside wall temperature to about 70°C.

The average reactor operating conditions are summarized in Table II .

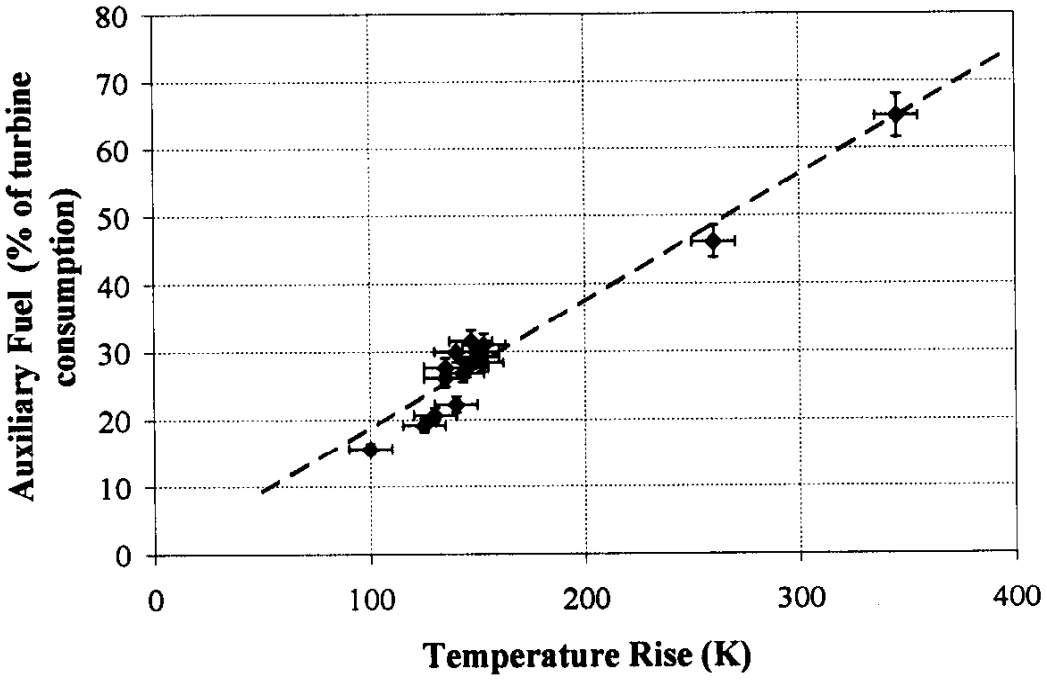

Figure 7. *Experimentally Observed Auxiliary Fuel Use (in Terms of Turbine Fuel Consumption) versus Temperature Rise. The initial temperature depends on turbine load, while the final temperature is maintained with auxiliary fuel injection in the range of 740 to 770 ℃.*

Reaction chamber at steady state full load conditions:	
Pressure loss	660 Pa
Mean final reactor temperature	700 – 780°C
Auxiliary fuel consumption	150 – 320 g/min
Residence time in recirculating zone	0.65 – 0.71 sec

Gas composition		
	before reactor	*after reactor*
O_2	15%	13.4 – 14.7%
CO_2	3.74 – 4.0%	4.2 – 5.2%
CO	380 ppm	30 – 150 ppm (T > 700°C)
NO_x	18 – 23 ppm (@15% O_2, dry)	20 – 34 ppm (@15% O_2, dry)
HC	60 -70 ppm	< 10 ppm

Table II. Average Reactor Operating Conditions (without NO Doping)

At steady state operation, CO and unburned HC emissions were reduced in the reactor from initial concentrations in the turbine exhaust to 30-120 ppm and ≤ 10 ppm, respectively (see Table II).

It was found that NO_x emissions increased by 10 – 15 ppm, when the reactor was brought to operating temperature. This increase appeared to be dependent on the amount of auxiliary fuel added and the corresponding average reactor temperature and independent of the initial NO_x level. The autoignition process of auxiliary fuel forms NO in the lean combustion zone and increases the net NO concentration by 10 – 15 ppm when no cyanuric acid was added. Since combustion of the injected auxiliary Diesel varied the O_2 content, all NO measurements are adjusted to 15% O_2.

3.3 NO_x Removal with Cyanuric Acid (CYA)

Figure 8 shows recorded data from a typical experiment. In the figure dry NO_x concentrations are shown as measured, and as adjusted to 15% O_2. These NO_x concentrations were obtained as a function of CYA added. The temperatures listed are the average temperatures in the recirculating section of the reactor. NO_x concentrations were allowed to reach steady state before any CYA feed rate changes were made. It can be seen that NO_x removal increases with increasing CYA injection. NO_x reduction from an initial concentration to as low as 18 ppm was achieved.

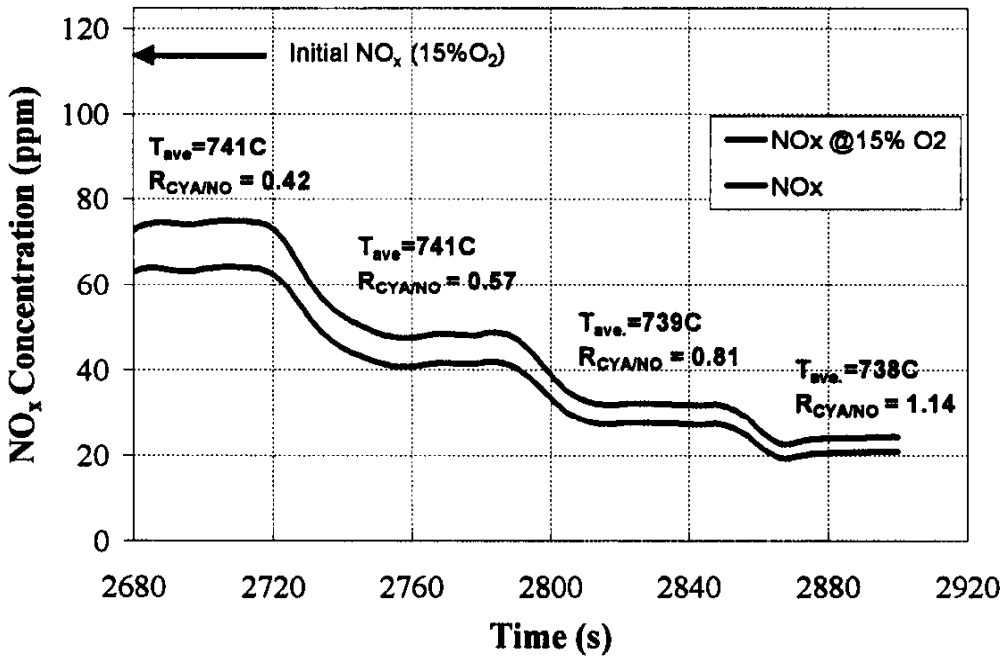

Figure 8. *NO_x Concentration Data versus CYA/NO_x Ratio at fixed Average Reactor Temperature.*

Highest NO reduction occurred at a CYA/NO_x ratio of 1.14 at 738°C. This ratio is higher than observed for gaseous isocyanic acid (HNCO), but value is in line with results from testing in a model gas turbine exhaust where insufficient residence time for cyanuric acid decomposition is available prior to NO reaction.

Figure 9 shows NO_x concentration at three molar CYA/NO_x ratios versus temperature. The plotted NO_x values are obtained by averaging steady state NO_x concentration data for each individual set of experimental parameters, similar to those seen in Figure 8. Here, CYA/NO_x ratios varied between 0.32 and 0.73. Temperatures range from 715°C to 785°C. The NO_x removal process improves with decreasing temperature and increasing CYA/NO_x ratio. A minimum of 34 ppm NO_x was observed. This minimum NO_x concentration corresponds to 71% reduction. Lowest efficiency was observed at a ratio of CYA/NO_x = 0.95 resulting in a NO_x concentration of 80 ppm, which equals 32% reduction. In all cases the initial NO_x concentration was 117 ppm +/- 2 ppm, and all concentrations are adjusted to 15% O_2.

Figure 10 shows measured NO_x concentration at turbine loads of 50, 75 and 100% versus CYA/NO_x ratio. The lowest NO_x emission of 26 ppm was found at maximum load and the highest CYA/NO_x ratio of 1.06. The process efficiency decreases with decreasing intake temperatures. Such a behavior is expected, since CYA sublimation and cracking to HNCO is less rapid at lower temperature. Compounding the effect is the mode of CYA injection. The slurry water, which surrounds the injected CYA charge, has to evaporate before individual CYA particles can be heated to sublimation.

Thus, with decreasing temperature, there is less CYA decomposed to HNCO. A smaller amount of HNCO provided to the recirculating reaction zone, decreases the amount of NO_x that is selectively reduced which results in a lower NO_x reduction efficiency. Since sublimation and cracking rates are exponentially dependent on temperature the effect seen here, is more pronounced at 50% load even though the temperature change to 75% load was equivalent to that from 75 to 100% load.

Commercial grade CYA has a grain size of less than approximately 400 micron. Additional grinding produced a grain size of the order of 100 micron. Since sublimation and cracking of the reagent is dependent on the square of the particle diameter, CYA powder size distribution can have a significant impact on the process efficiency. The encountered high CYA/NO_x ratios might be explained by insufficient decomposition of the CYA ($(HNCO)_3$) to the isocyanic acid (HNCO). If particle size is process limiting, smaller reagent particle size should result in decreased CYA/NO_x ratios.

In Figure 11 various reagent compositions are compared at 100% load. The resulting NO_x reductions appear to be independent of the make up of the constituents of the slurry. These results indicate that neither particle size nor purity are responsible for the observed high CYA/NO_x ratios.

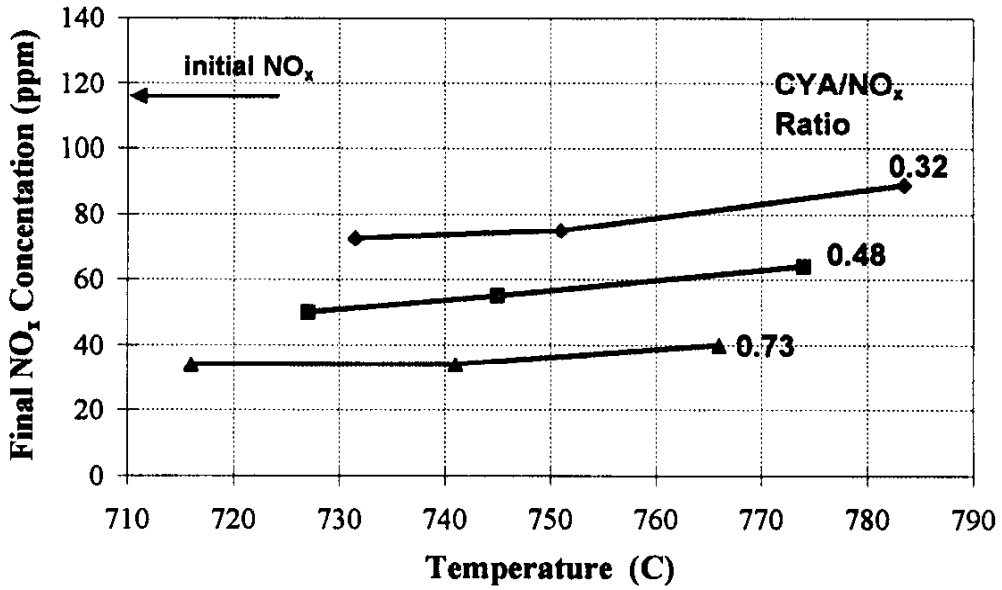

Figure 9. *NO_x Concentrations versus Average Reactor Temperature and CYA/NO_x ratios of 0.32, 0.48 and 0.73. All NO_x measurements are adjusted to 15% O_2 content. Turbine exhaust temperature (reactor intake temperature) was 610℃.*

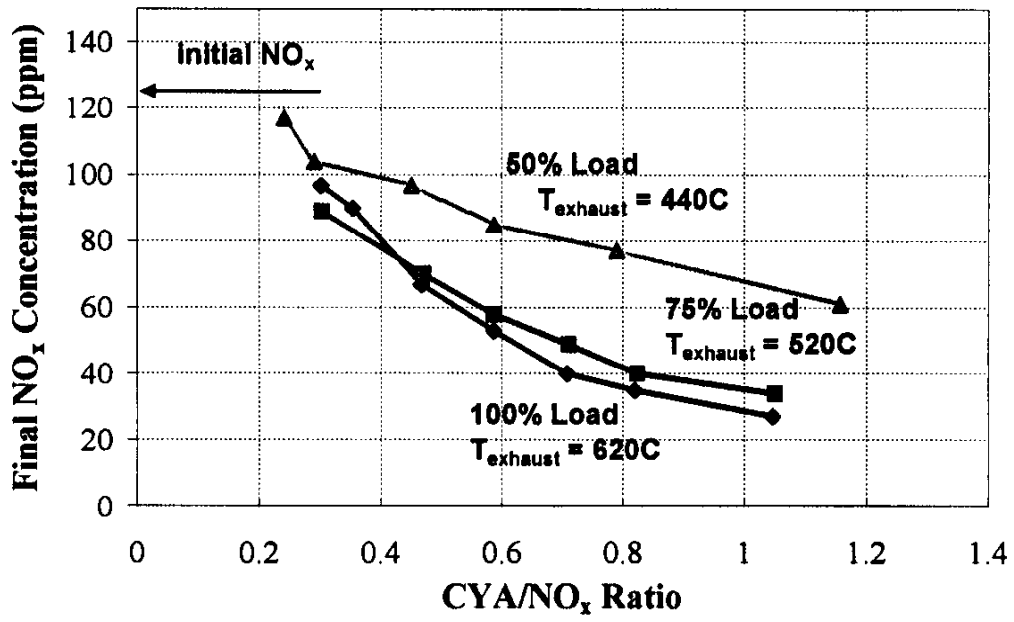

Figure 10. *Final NO_x (at 15% O_2) Concentration versus CYA/NO_x Ratio and Temperature at Turbine Loads of 50, 75 and 100%.*

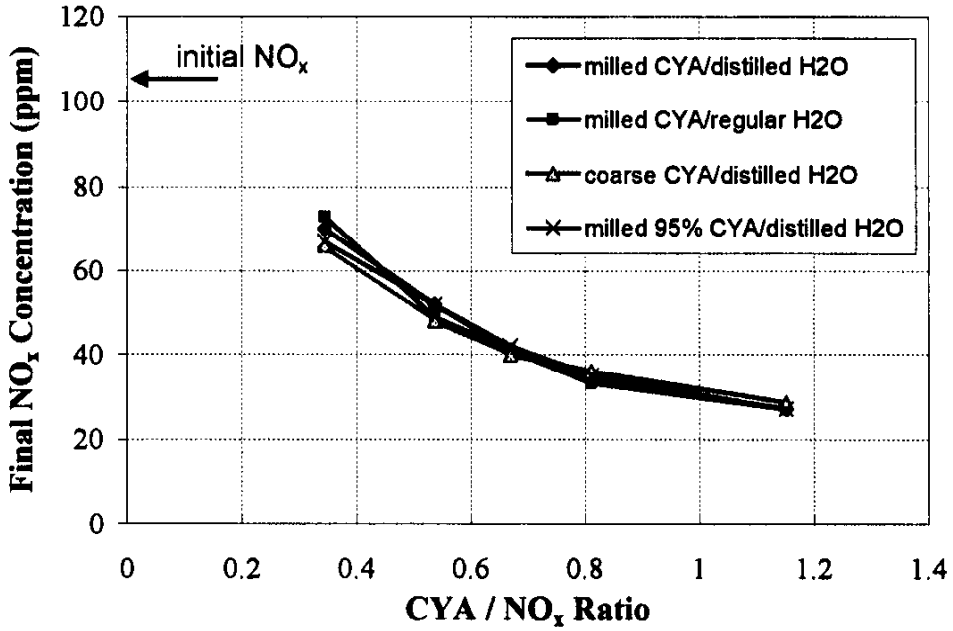

Figure 11. NO_x Reduction versus CYA Grain Size and Slurry Composition. Commercial CYA powder is compared with milled CYA powder of smaller grain size, both mixed with distilled or regular water.

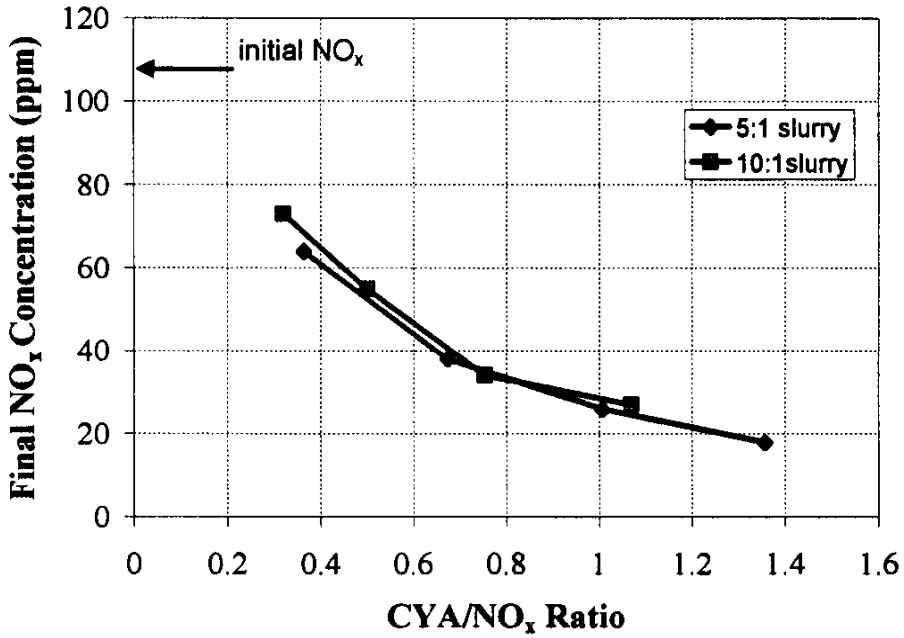

Figure 12. *NO_x Reduction versus CYA/NO_x Ratio and Slurry Water Content. The slurry composition ratios are based on mass of water to mass of CYA.*

In order to evaporate the slurry water, to sublime CYA and to decompose CYA to HNCO, significant energy (i.e heat) has to be transferred to the injected CYA slurry. One possibility to reduce the amount of energy necessary to evaporate and heat the added water is to reduce the amount of water in the slurry. Further tests compared performance of a 5:1 slurry (5 parts water to 1 part CYA by mass) to that of the usually used 10:1 slurry feedstock. Figure 12 shows that both slurry compositions are equally effective in removing NO_x. The lowest No_x value of 18 ppm was obtained for these experiments.

Measurements of CYA or NH_3 slip and N_2O were obtained while operating at steady state for various conditions at 100% load. Neither HNCO nor NH_3 were found in the flue gas stream leaving the reactor. Within the limits of detection uncertainty, CYA (i.e. HNCO) slip was determined to be less than 10 ppm. Thus HNCO and NH_3 slip is negligible.

In Figure 13, measured N_2O concentrations with respect to CYA/NO_x ratio are shown. A clear increase with increasing CYA/NO_x ratio can be seen. At a molar ratio of $CYA/NO_x = 0.33$, 46.5 ppm of N_2O are found while at a CYA/NO_x ratio of 1.08 as much as 166 ppm are observed. A possible mechanism in which CYA decomposes and in part forms NO, to be subsequently reduced to produce N_2O, could explain these observations. Such a decomposition of $(HNCO)_3$ would also provide an explanation for the high CYA/NO_x ratios as seen in these tests. Since neither insufficient sublimation and cracking nor mixing were found to influence the amount of CYA required, the theoretical decomposition of CYA to 3 molecules of HNCO is most likely incorrect for this experimental setup. What can be concluded is that part of the injected CYA decomposes to HNCO, which in turn reduces NO. The fate of the remainder is not clear and requires further investigation.

As part of a check on reaction efficiency, and in order to compare the use of ammonia with the recirculating reactor to cyanuric acid use, we injection ammonia instead of cyanuric acid for certain experiments. As noted in Figure 14, ammonia injection prior to the reactor resulted in a major increase in NOx production (rather than reduction) when ammonia was introduced. (Clearly ammonia was not acting like cyanuric acid in this reactor, although it should be noted that amine impurities in the cyanuric acid might react similar to ammonia to reduce the effectiveness of the process.)

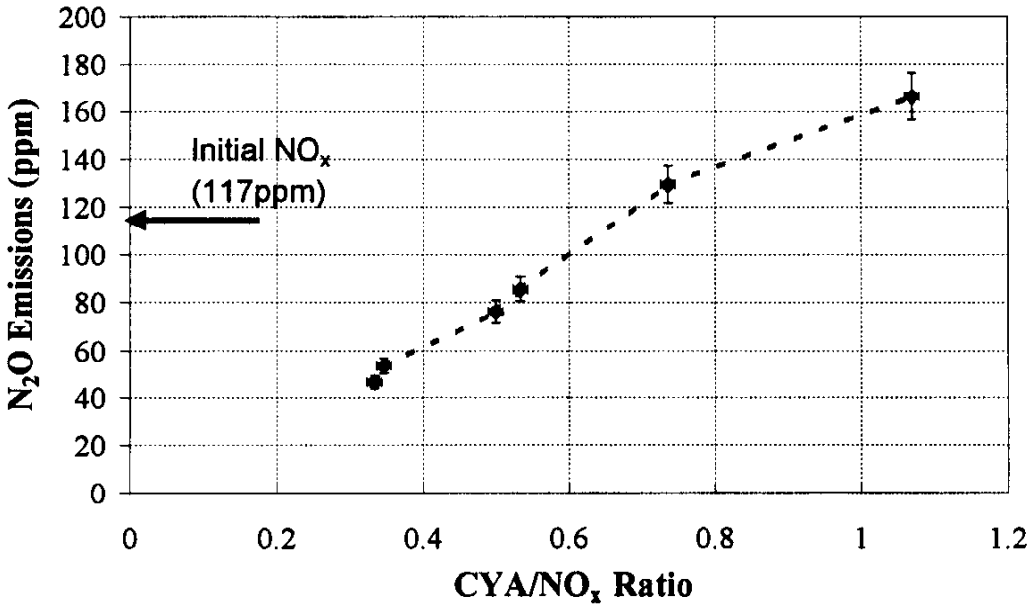

Figure 13. *N_2O Concentration adjusted to 15% O_2 (dry) versus CYA/NO_x Ratio at Average Reactor Temperatures of 715 – 725°C and 100% load.*

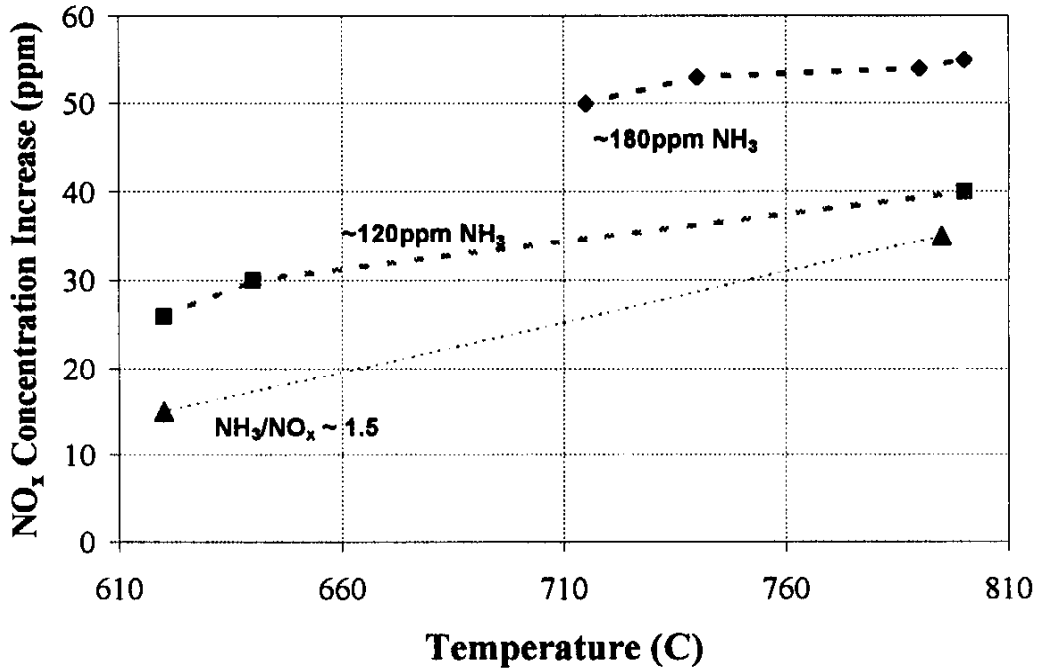

Figure 14. *NO_x Concentration Increase with NH_3 Addition versus Reactor Temperature. Data are shown for different NH_3 concentrations or NH_3/NO_x ratios. Inlet NO_x concentration varied between 40 and 120 ppm*

4.0 Numerical Modeling

The description of a non-reacting flow requires the solution of the three-dimensional Navier-Stokes equations. Currently, computational resources do not allow modeling of three-dimensional fluid dynamics coupled with full chemical kinetics for a reactor of this scale. One is therefore forced to make simplifying, enabling assumptions. A choice has to be made whether the emphasis should be on a detailed description of the fluid dynamics combined with a set of global chemical reactions or on the detailed formulation of the complex chemical kinetics with simplified fluid dynamics. Both modeling approaches are challenging.

Since most flows of interest are turbulent, detailed fluid dynamic modeling often becomes impractical. In contrast, detailed chemical kinetic models with simplified fluid dynamics have achieved practical results for a variety of technical applications in reasonable time, without extravagant computational means.

Gas phase selective NO_x reduction, is largely a chemical kinetic dominated process and thus, the focus of the modeling effort is on detailed chemistry. The goal hereby is to gain a better understanding of the reaction kinetics and find the theoretical process potential, as well as its limitations. Particular attention is given to the modeling of autoignition through recirculation and simultaneous NO_x reduction.

4.1 Model Description

In the experiment, a lean premixed flow of air, fuel and reactant interacts with the hot product flow inside the recirculation zone. The hot products act as ignition source for the incoming cooler stream and thereby stabilize the reaction. This scenario is encountered whenever a lean premixed combustion process is stabilized with the means of a turbulent recirculation zone. The description of such a lean premixed combustion process has been achieved for the purpose of modeling a gas turbine combustor by a combination of a perfectly stirred reactor (PSR) and a plug flow reactor (PFR).[2,3] Using a set of such idealized reactors in series permits the detailed description of the chemical kinetic phenomena. A schematic of this commonly used reactor sequence is shown below in Figure 15.

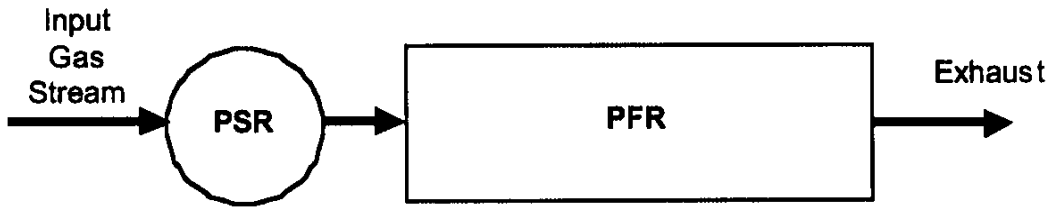

Figure 15. PSR in Series with PFR. Typically, ignition is achieved in the PSR while burnout occurs in the PFR to model a reacting flow stabilized by a turbulent recirculation zone.

The output of the PSR provides the input to the PFR. In contrast to the turbulent combustion inside a gas turbine, where this model finds its principle use, the process investigated here, occurs inside a large recirculation zone, the entry section of the reaction chamber. The goal therefore is not so much to model the recirculation zone with subsequent burnout inside the stack but to model the recirculation zone itself. To do that, a significant amount of the final product of the reaction inside the chamber is brought into the initial PSR to interact with the incoming mixture. A simple combination of PSR and PFR does not incorporate this important feature. Therefore, a new model has been developed, the so-called PSRPFRX, in which a fraction of the output of the PFR recirculates to be input alongside of the fresh reactant mixture in the PSR (shown below).

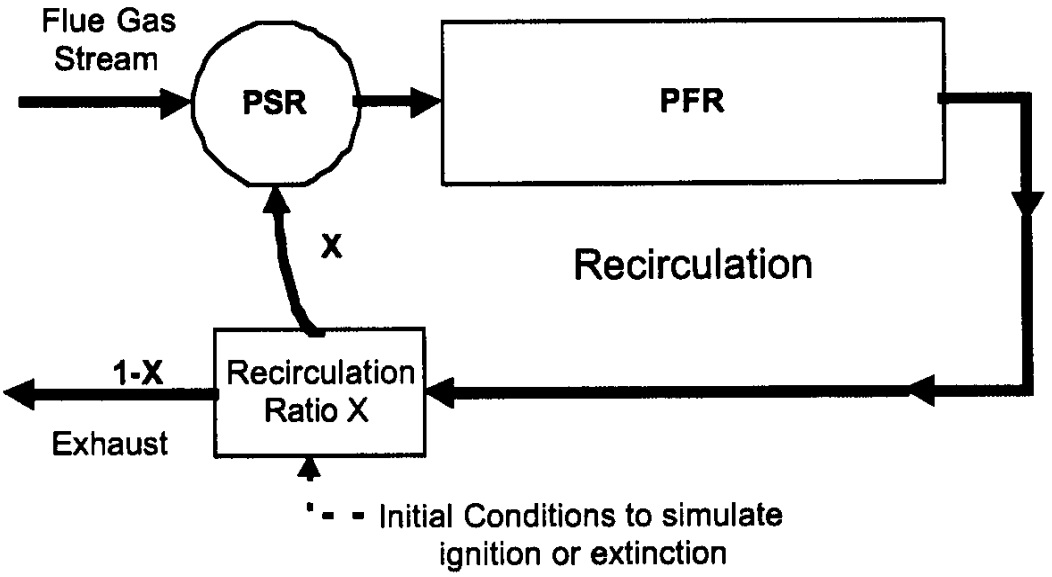

Figure 16. Schematic of the PSRPFRX Algorithm. A part of the output form the combination of PSR and PFR is injected into the PSR alongside of the incoming stream.

Adjusting the parameter X varies the amount of recirculation. The initial conditions of the reactor can be input, which allows the modeling of initial

ignition in a 'cold ' reactor as well as extinction of an operating 'hot' reactor. Setting initial reactor temperature and gas composition equal to turbine exhaust gas temperature and composition simulates autoignition in a 'cold' reactor.

PSR and PFR models run in conjunction with CHEMKIN, a software package that handles all chemical reactions and the necessary thermodynamics.[4] It requires a detailed chemical mechanism and a corresponding thermodynamic data file in JANAF format .[5]

Efforts have been made to build and continuously improve detailed chemical kinetic mechanisms, which describe the chemistry in a variety of combustion scenarios. These mechanisms consist of a number of elementary reactions and their characteristic Arrhenius coefficients. The amount of elementary reactions necessary to describe a global chemical reaction, depends in general on the complexity of the used reagents and the level of detail desired. Due to the complexity of Diesel combustion, the calculations were made using propane as the fuel of choice

To test the validity of this propane based approach, experiments were performed in which propane was the auxiliary injected fuel. The experimentally obtained results showed that for the described purposes propane and Diesel fuel are interchangeable. Similar autoignition characteristics as well as comparable NO_x reduction was achieved. The reactor model of this study, used a mechanism developed by Westbrook and Pitz[6] for propane and propene oxidation, which has been found to properly describe very fuel lean scenarios ($\Phi \sim 0.05$). To handle NH_3, HNCO and NO_x chemistry, this set of reactions was combined with a nitrogen chemistry mechanism by Miller and Perry .[7] In total, 69 species and 311 elementary reactions are considered.

4.2 Modeling Results – NO_x Reduction with CYA

There are two main objectives in the modeling effort of this study. One is to explore the effect of recirculation, combined with combustion and heat release on the NO_x reduction chemistry and the other, to find the theoretical process potential and the effect of the various process parameters such as temperature and reagent to NO ratio on its performance.

The first objective is approached by comparing NO_x reduction results from a PFR with those obtained from the PSRPFRX algorithm with propane addition. The second objective is achieved by variation of fuel and reagent input into the PSRPFRX reactor model. In both cases recirculation ratio X = 30% and the used propane chemical mechanism is that of Westbrook and Pitz.[6] In all cases it is assumed that cyanuric acid has been sublimed and cracked to form gaseous HNCO, before entering the reactor.

4.2.1 The Effect of Hydrocarbon Oxidation on the NO Reduction with CYA

In the case where a process reagent is added to previously heated exhaust, a PFR model has been used. Final NO_x concentrations versus temperature plots, shown by the broken lines in Figure 17, have been obtained for $HNCO/NO_x$ ratios of 1, 1.5 and 2 at 1 second residence time. They are contrasted to final NO_x concentrations from a combined propane addition, autoignition and NO_x removal in a recirculation zone simulated with a PSRPFRX model (solid lines). For the conventional PFR reduction process (broken lines), significant reduction of more than 84% is predicted at 780°C and a molar HNCO/NO ratio of 1. The temperature windows were found to increase in width with increasing HNCO/NO ratio.

It is interesting to note that at each temperature a specific ratio predicts the lowest NO_x concentration, or in other words, has the highest NO_x reduction potential. These ratios are increasing with increasing temperature. The lowest (PSRPFRX) NO_x concentration here are found to be 8.3 ppm at a $HNCO/NO_x$ ratio of 1.5 and a temperature of 730°C. Minimum values of NO_x of 22.3 ppm and 16.4 ppm at HNCO/NO ratios of 1 at 783°C, and 2 at 853°C, respectively, are predicted. All values are obtained for an exhaust gas composition of 15% O_2, 4% CO_2, 3.6% H_2O, 200 ppm CO and 140 ppm NO_x balanced with nitrogen. In contrast to these PFR model results, addition of fuel, heat release and recirculation appear to enhance NO_x reduction performance and lower the required temperature. NO_x reduction increases with decreasing temperature and achieves a minimum of 1.6 ppm NO_x at a HNCO/NO ratio of 2 and a temperature of 741°C.

The temperature is 110°C lower than that observed in the PFR model scenario. Similarly to the conventional use of CYA, NO_x reduction performance increases with increased HNCO/NO ratio. Modeling the combination of auxiliary fuel combustion and NO_x removal results in improved reduction effectiveness, significantly lower temperature and energy requirement and reduced residence time (i.e. reactor size in a practical system).

4.2.2 The Effects of Temperature and HNCO/NO Ratio

A gas composition similar to that seen in the experiment is heated by addition of propane, at equivalence ratios of 0.053, 0.060, 0.067, 0.075 and 0.0852. The resulting temperatures are 727, 740, 751, 767 and 785°C +/-1.5°C, respectively, given an exhaust gas inlet temperature of 627°C. The HNCO/NO ratio is varied from 1 to 3. Figure 18 shows the resulting NO_x concentrations. A trend of increasing NO_x removal efficiency with increasing HNCO/NO ratio is seen. A minimum value of 3.3 ppm NO_x is found at a HNCO/NO ratio of 3 and a temperature of 741°C.

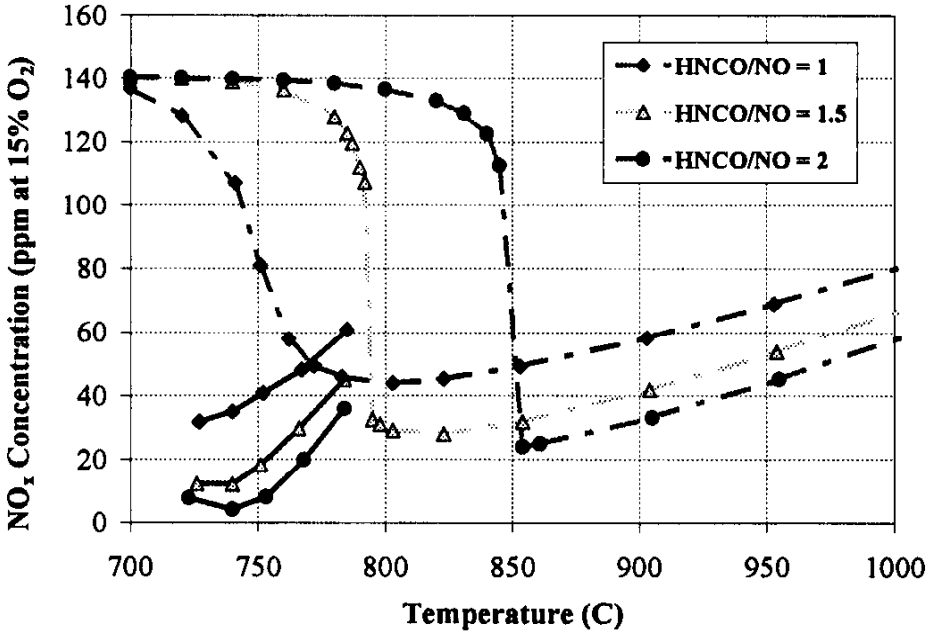

Figure 17. *Model Results of NO_x Removal for Different HNCO/NO Ratios. Solid lines = propane addition; broken lines = without propane addition*

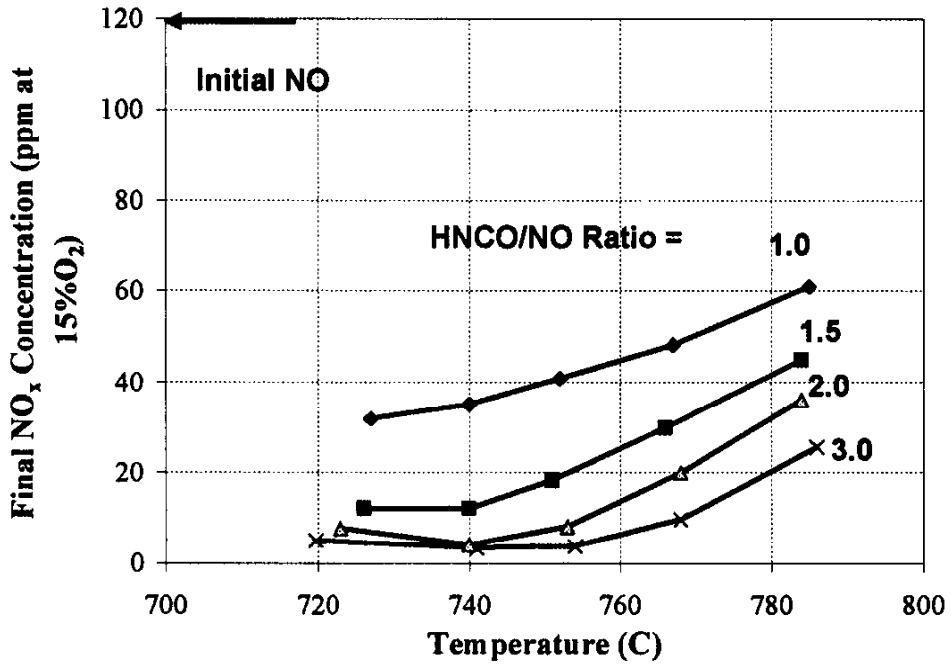

Figure 18. *Final NO_x Concentration versus Temperature and HNCO/NO Ratio. Initial exhaust gas composition includes 15% O_2, 3.8% CO_2, 3.5% H_2O, 300 ppm CO, 120 ppm NO and the corresponding HNCO and propane concentration balanced with nitrogen.*

The highest process efficiency for the HNCO/NO ratio of 2 with a maximum reduction to 4.1 ppm NO_x is found at a temperature of 740°C. Both ratios of 2 and 3 exhibit peak performance in terms of NO_x removal at the same temperature. Significant reduction from 120 ppm NO_x to a minimum value of 31.8 ppm is found for the HNCO/NO ratio of unity at a temperature of 723°C.

4.2.3 N_2O Formation

The most important process byproduct is N_2O. Figure 19 shows final N_2O concentration versus temperature and HNCO/NO ratio. A maximum of 74 ppm N_2O at a ratio of 3 and a temperature of 755°C is observed. The amount of N_2O formed increases with the addition of HNCO and decreases slightly with temperature above 740°C to 755°C depending on HNCO/NO ratio.

N_2O formation peaks at a temperature of 740°C and an HNCO/NO ratio of 2 and 1.5. At a ratio of 1, the highest value is found at 727°C. The minimum value of N_2O is 20 ppm at a HNCO/NO ratio of unity and a temperature of 785°C.

4.3 Modeling Results- NO Reduction with Ammonia

A check on the model was made by calculating results for the addition of NH3 to the exhaust gases. Similar to model of isocyanic acid addition, reagent (NH3) and fuel are added to the exhaust gases prior to entry into the recirculating reactor. Recirculation rate is fixed at X = 30% and all other conditions, such as exhaust gas composition and equivalence ratio, remain the same.In every case, NH_3 addition led to a net increase of the initial NO_x concentration, i.e. instead of reduction, formation is encountered. In Figure 20, resulting NO_x concentrations versus temperature and NH_3/NO ratio are plotted. The observed amount of NO_2 ranges in between 8 and 15% of the total NO_x. Increased NH_3/NO ratio leads to increased NO_x formation. The largest value of 293 ppm NO_x is found at a NH_3/NO ratio of 3 and a temperature of 727°C. Since the equivalent of 360 ppm NH_3 has been added these findings suggest a peak NH_3/NO_x conversion of 76%.

In summary, it can be concluded that the application of NH_3 as NO_x reducing reagent in a recirculating reactor model with simultaneous fuel injection, leads to NO formation instead of reduction. Fuel combustion when combined with ammonia injection leads to direct oxidation of the ammonia to NO.

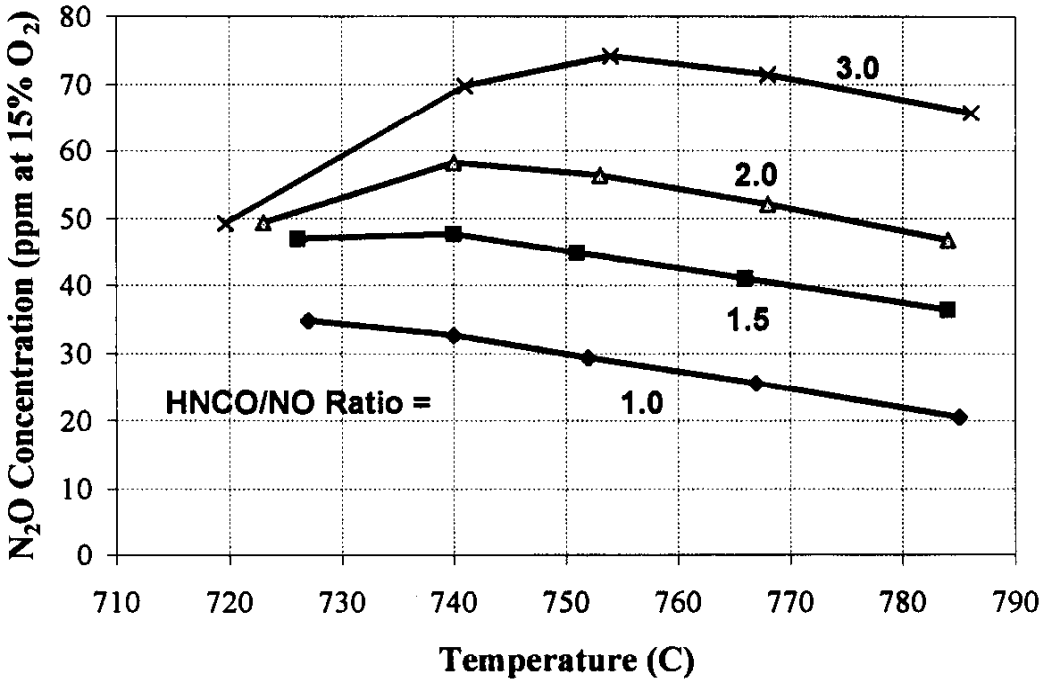

Figure 19. *N_2O Formation versus Temperature and HNCO/NO Ratio. The initial NO concentration is 120 ppm and the exhaust gas temperature 627℃.*

5.0 Comparison of Experiment and Model

5.1 Additional Fuel Consumption

It is instructive to compare the calculated and measured fuel consumption for the process. The numerical model assumes adiabatic conditions and any auxiliary fuel input therefore produces ideal final reactor temperatures. In the experiment, fuel was added such, that the desired process temperature was reached. Figure 21 compares the theoretical, ideal values with those obtained when operating the reactor. Reactor inlet temperature in the model is 600°C, which corresponds to the average inlet temperature observed in the experiments. Under ideal circumstances, i.e. no heat loss, the model predicts between 15.5 and 29% additional fuel injection to heat an exhaust gas stream with an initial temperature of 600°C, to a process temperature of 700 to 791°C, respectively. The experimental values are higher.

At final temperatures of 740 to 750°C, 5 to 7% more auxiliary fuel is consumed than in the model. With the large surface area of the reactor and an outside surface temperature of 40 – 80°C heat losses of this order are expected. With an overall limited heat loss of 5 to 7%, approximately adiabatic conditions can be claimed.

5.2 Residence Times for Autoignition

The numerical ignition delay times vary considerably depending on recirculation ratio, entry temperature and the chemical mechanism employed. In the experiment, the reactor is found to support steady state operation at a residence time of less than 0.71 seconds and incoming exhaust temperatures above 440°C. The Westbrook and Pitz[6] model predicts residence times of 8.4 to 4.4 seconds in a temperature range of 577 to 627°C.

The observed disparity between the experimental and the numerically derived values can be explained by the complex nature of hydrocarbon pyrolysis, as discussed earlier. With the advent of mechanisms that specifically address propane autoignition at equivalence ratios below 0.1, this apparent discrepancy may be reconciled. However, the predicted trends agree with the experimental trends.

Initial reactor geometries did not promote as much recirculation as the final version discussed here. Autoignition with entry temperatures lower than 610°C was not achieved. Upon installing the described partitions, to achieve significant recirculation, steady state was approached rapidly and the temperature range of operation expanded. With the present optimized reactor geometry, extinction does not occur inside the reactor until intake temperatures fall below approximately 440°C.

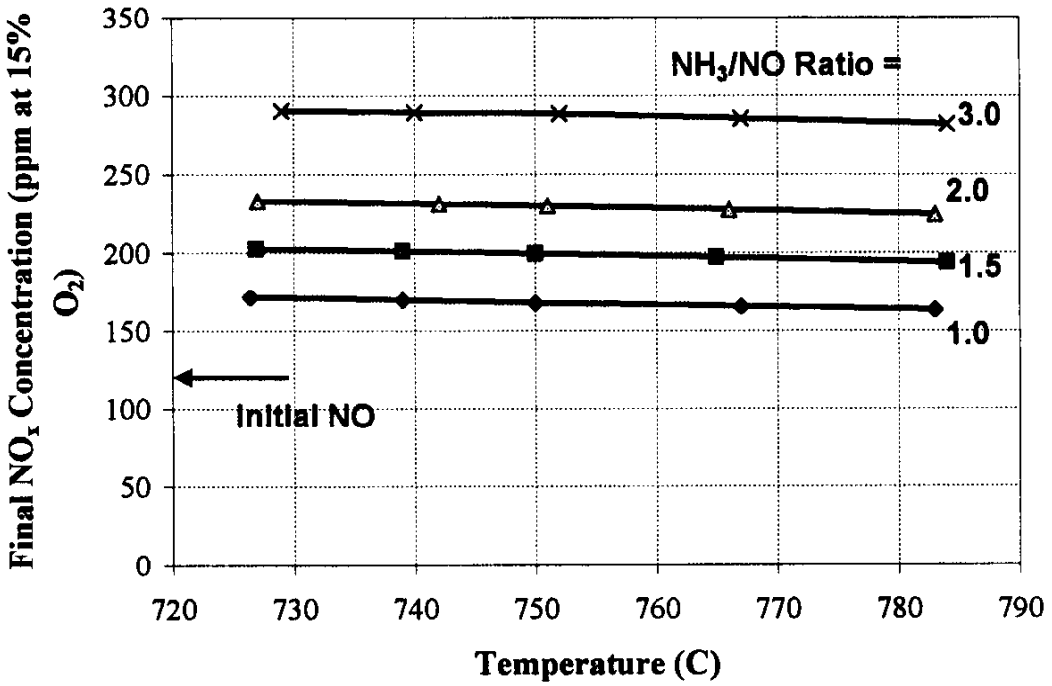

Figure 20. *Final NO_x Concentration versus Temperature and NH_3/NO Ratio. Initial exhaust gas composition: 15% O_2, 3.8% CO_2, 3.5% H_2O, 300 ppm CO, 120 ppm NO.*

5.3 NO_x Removal with CYA

When comparing experimental and numerical NO_x reduction with cyanuric acid, the assumption that the thermal decomposition of CYA yields three molecules of isocyanic acid, HNCO, is used.

In Figure 22, NO_x concentration versus temperature and reagent/NO_x ratio are shown. Experimental and numerical curves for constant reagent addition, are similar in shape but shifted. The experimental NO_x concentrations are in every case higher than the numerical values, corresponding to an over prediction of NO_x reduction by 21 to 27%. Besides this obvious disparity in absolute NO_x values, the general agreement between the modeled and observed trends is good. Increasing NO_x removal with increasing reagent injection and the temperature dependence is properly modeled. The model captures the apparent maximum in NO_x reduction at 740°C for a CYA/NO_x ratio of 0.73 (which corresponds to a numerical HNCO/NO ratio of 2.2). The relative differences between the resulting NO_x concentration as a function of temperature and reagent/NO_x ratio are similarly replicated.

A comparison of NO_x removal versus CYA/NO_x ratio at a fixed average temperature of 740 to 750°C reveals a similar result, as shown in Figure 23 Although there is an approximate 20 ppm disagreement in NO_x values, corresponding to an over prediction in NO_x removal of 11 to 21%, experimentally observed trends are replicated well by the model. The rate of numerical NO_x concentration decrease, with respect to CYA/NO_x, ratio properly matches the experimental observations.

Investigation of the effect of reactor inlet (= turbine exit) temperature on the NO_x reduction chemistry is central to the issue of turbine load following. The final NO_x concentrations, obtained by numerical and experimental variation of reactor inlet temperatures, are contrasted in Figure 24. The numerical values are based on initial experimental conditions, such as exhaust gas composition and temperature measured at 50, 75 and 100% turbine load.

The numerical differences in NO_x reduction between initial conditions generated by 50 and 100% load are of the order of 5 to 15%.

Experimentally, a much larger discrepancy is observed. The model predicts better than 50 to 90% NO_x reduction with a CYA/NO_x ratio of 0.33 to 1.0, respectively. Similarly to the previous results, the model agrees well with the overall behavior but does not reproduce the exact NO_x concentration values. A difference of as much as 47% at the lowest CYA/NO_x ratio and 20% at the highest CYA/NO_x ratio, at 100% load, is seen.

As discussed earlier, this phenomenon can be explained by insufficient sublimation and cracking of the injected reagent prior to entry in the recirculation zone.

9.3.2 N_2O Formation

When the experimentally obtained N_2O concentrations are compared to the modeled N_2O concentrations, agreement between model and experiment is not as good. As shown in Figure 25, N_2O concentrations deviate by as much as a

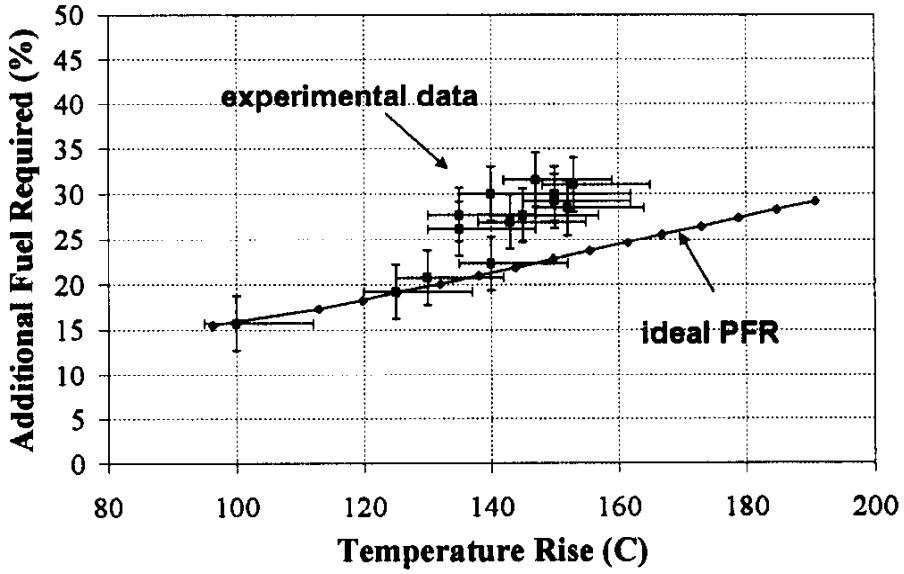

Figure 21. *Comparison of Experimental and Theoretical Additional Fuel Consumption. The theoretical values were obtained with exhaust gas composition similar to the experiment and an entry temperature of 600℃ at adiabatic conditions.*

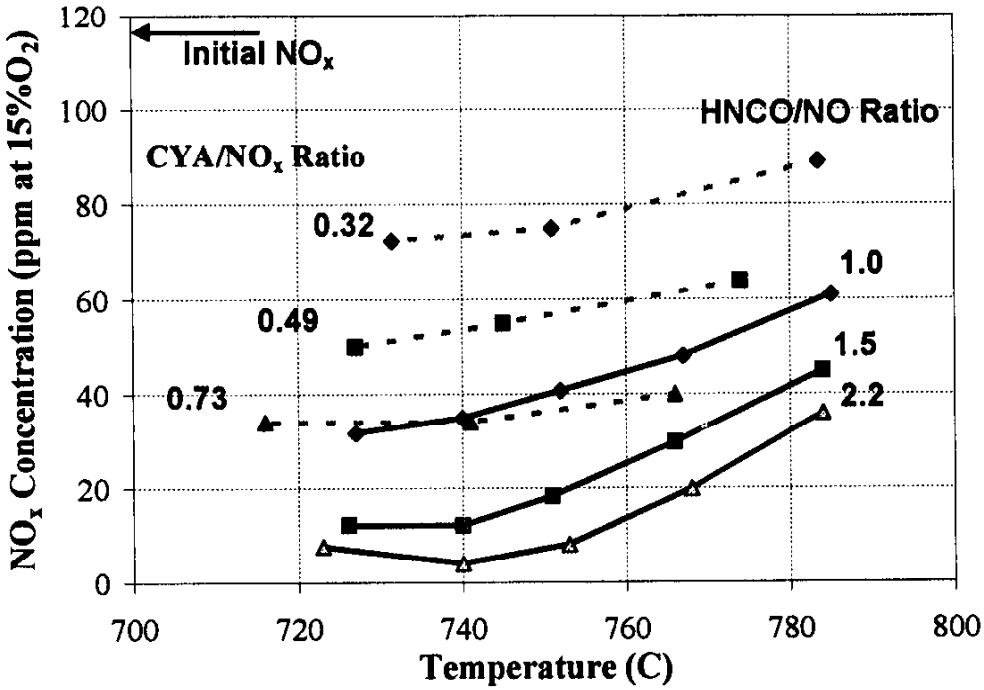

Figure 22. *Comparison of Experimental and Numerical NO_x Reduction with CYA. The solid lines are numerical values while the broken lines represent experimental results. The experimental and numerical reagent/NO_x ratios are indicated on the left and right respectively.*

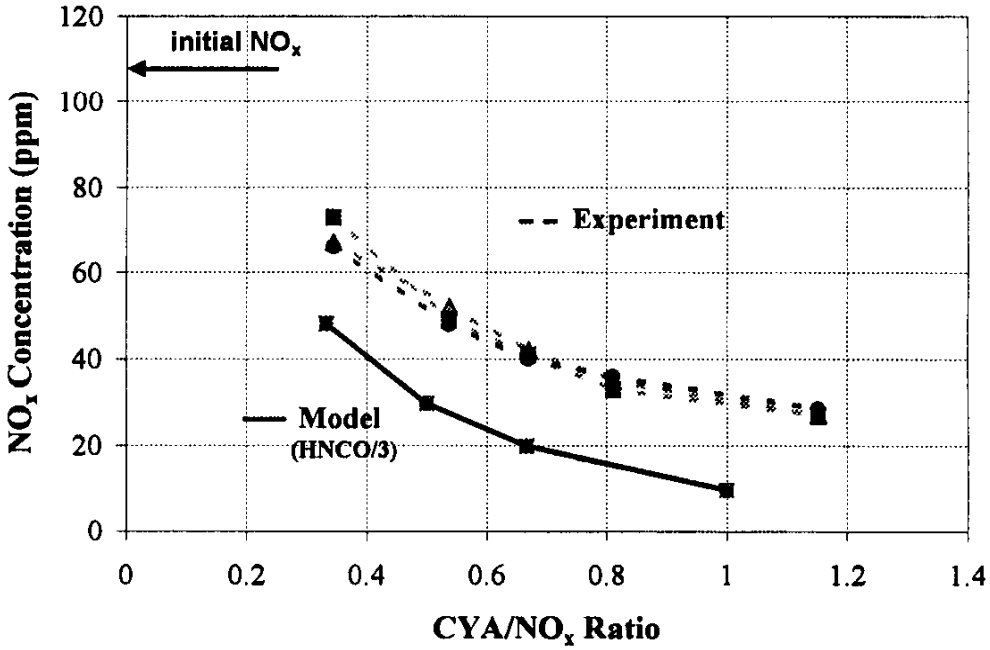

Figure 23. *NO_x Removal at Fixed Temperature versus CYA/NO_x Ratio. Experiments were performed at an average temperature of 750°C at 100% turbine load.*

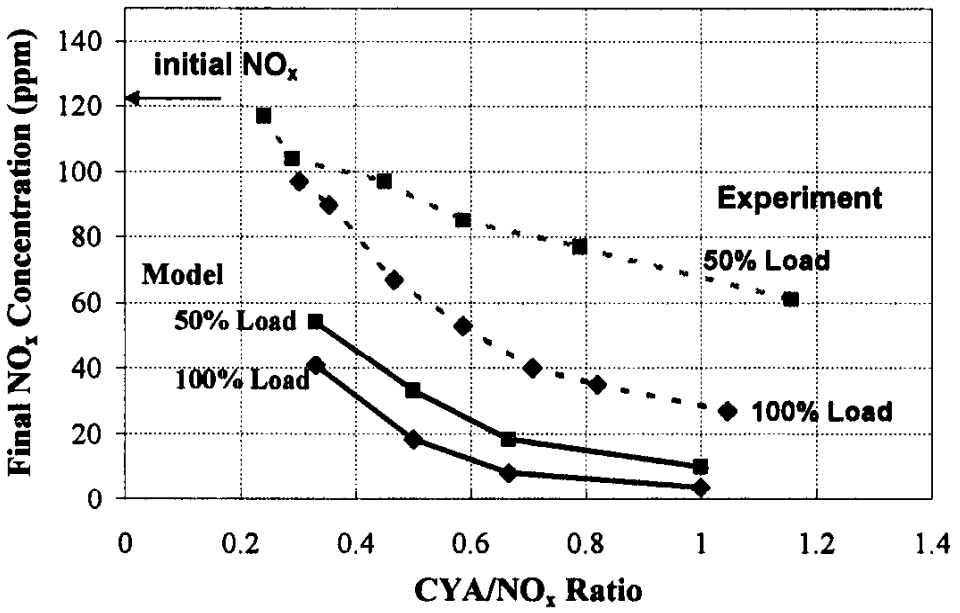

Figure 24. NO_x Concentration versus Turbine Load; Numerical and Experimental Values. Final reactor temperature remained fixed at 760°C (+/- 10°C), while the intake temperature varied with turbine load. A load of 50%, 75% and 100% corresponds to 440°C, 520°C and 610°C respectively.

factor of 3. All plotted values are adjusted to 15% O_2. As before, observed reactor temperatures are input into the model, so that initial experimental conditions are simulated. The model only in part captures the trend of increasing N_2O emissions with increasing CYA/NO_x ratio. Numerical N_2O emissions appear to plateau at approximately 50 ppm independent of CYA/NO_x ratio,
while the experimental values increase with reagent ratio. The maximum N_2O concentration measured exceeds the initial NO_x concentration in the turbine exhaust. Since N_2O formation is primarily a byproduct of the NO reduction along the NCO + NO pathway , detected N_2O cannot be a result of conversion of the initial NO concentration alone. Another pathway to explain these emissions has to be active. Further evidence for the existence of a mechanism not considered by the model is provided by Figure 25. Measured concentrations of "N_2O formed" versus "NO_x reduced" are compared to the values determined by the numerical model.

Experimental N_2O emissions follow an approximate 1.5 to 1.0 ratio of "N_2O formed" to "NO removed". In contrast, modeling results are clustered about a slope of 0.3 to 0.5. The needed CYA/NO_x ratios, i.e. 3HNCO/NO_x ratios, (of ~1), to achieve maximum reduction are significantly higher than the observed CYA/NO_x ratios for gaseous isocyanic acid injection[8] but in agreement with the results from a model gas turbine combustor.

The assumption used by the model is 'perfect' thermal decomposition of cyanuric acid to three molecules of HNCO. The phenomena seen here might be explained by a possible mechanism, that reduces the effective conversion of cyanuric acid to isocyanic acid in a lean-burn conditions.

$$(HNCO)_3 + OH \Rightarrow (HNCO)_2NCO + H_2O \quad (1)$$

$$(HNCO)_2NCO + O_2 \Rightarrow (HNCO)_2NCO(O_2) \text{ (Adduct)} \quad (2)$$

$$(HNCO)_2NCO(O_2) \text{ (Adduct)} \Rightarrow 2HNCO + NO + CO_2 \quad (3)$$

This mechanism would predict the experimentally needed CYA/NO_x ratio (of ~1) to reduce NO and the higher production of N_2O when using slurry based CYA injection. To incorporate this alternative decomposition path into the model, additional chemical kinetic data and an associated branching ratio is required.

5.4 The Use of Ammonia as a Process Reagent

The experimental use of NH_3 in the recirculating reactor led to a significant increase in NO_x concentrations in the flue gases, while NH_3 slip was not detected. The numerical model, as shown in Figure 26, replicates these experimental findings.

In the PSRPFRX model, NH_3 is entirely consumed and partially oxidized to NO, leading to an increased NO_x concentration. The model also predicts a slight decrease in NO formation with increasing temperature. In the experiment the decrease is not noticeable. Besides that, the model agrees well with the experimental results.

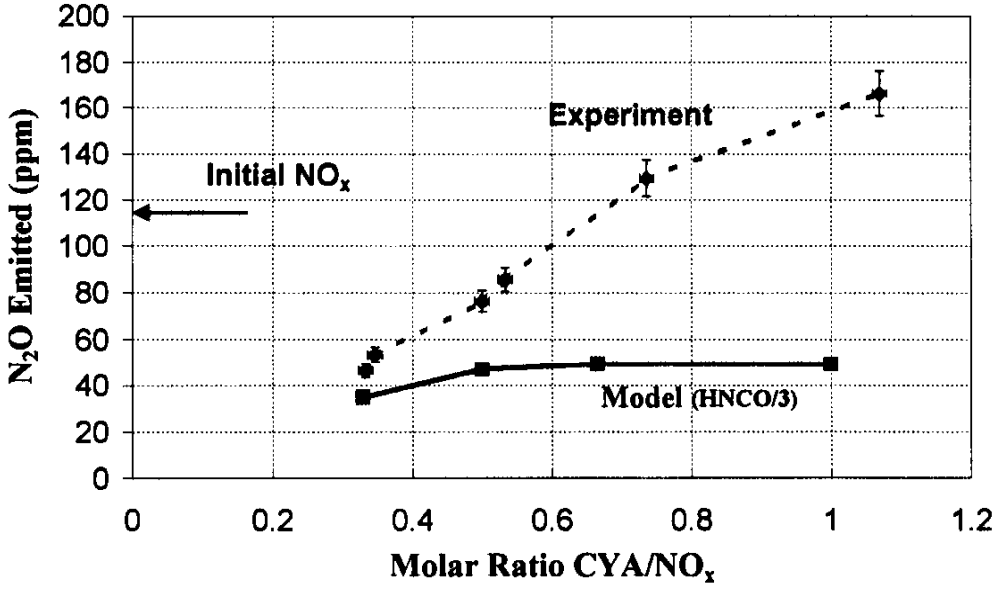

Figure 25. *Experimental and Numerical N_2O Emissions versus CYA to NO_x Ratio. The reagent to NO ratio of the model is adjusted corresponding to CYA = 3 HNCO. Initial conditions such as temperature and exhaust gas composition, are similar.*

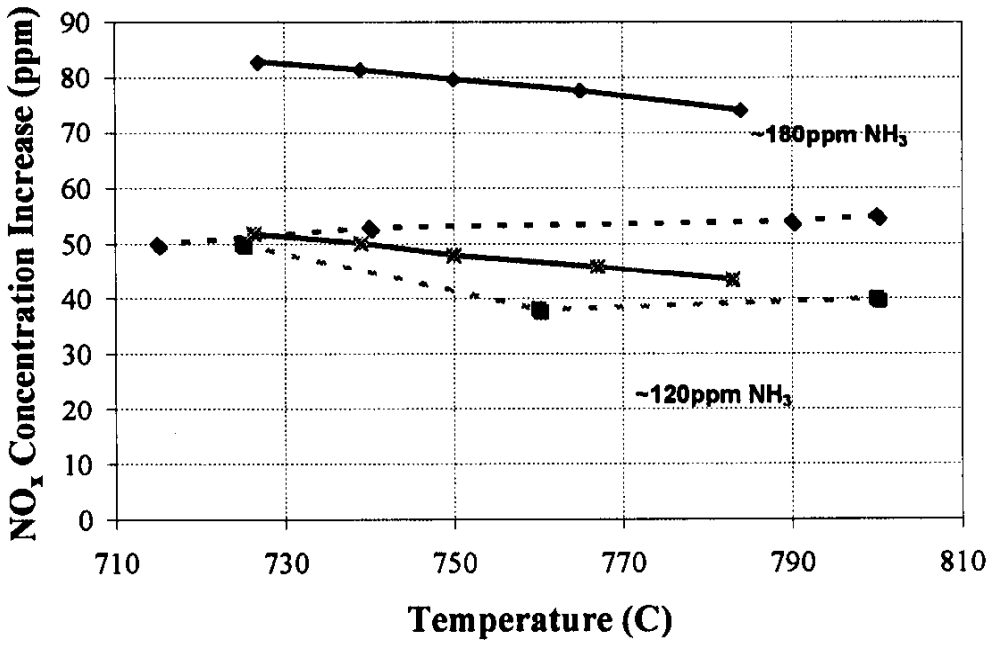

Figure 26. *Experimental and Numerical NO_x Increase due to Injection of NH_3. Solid lines represent numerical results while broken lines connect experimental values. The experimental conditions varied in initial NO_x concentration between 40 and 120 ppm NO_x; the absolute increase was found to be solely a function of NH_3 injection rate.*

5.5 Summary

The overall agreement between experimental findings and numerical simulation is good. All trends are properly featured in the model. Given that the model does not consider sublimation and decomposition of the injected reagents and ignores mixing as well as three-dimensional turbulent fluid dynamics, the agreement is remarkable.

The model therefore allows meaningful predictions of NO_x reduction potential with respect to temperature and reagent injection rate of cyanuric acid. As indicated, solid reagent decomposition might be responsible for the discrepancies in absolute NO_x and N_2O concentrations modeled and observed. In previous research, Perry[9] reported relatively lower N_2O emissions and $HNCO/NO_x$ ratios of 1.4 to 1.6, when injecting HNCO in gaseous form into the effluents of a Diesel engine.

Prior gasification of CYA and subsequent decomposition are technically challenging in an industrial scale application. A possible delivery system is suggested which combines the use of an easily controllable flow of slurry with subsequent vaporization of the water, sublimation and thermal decomposition of CYA. By insertion of this system into the exhaust gases coming from the reactor, no additional heat input would be required.

Other means of reducing N_2O emissions, caused by the CYA process, might also be employed. Miller and Perry[7] propose the introduction of alkali metals into the CYA reduction scheme. N_2O emissions were significantly reduced in the presence of NaOH.

6.0 TECHNICAL AND ECONOMIC SUMMARY

Based upon the results of this testing an on the projected cost associated with operation on a Allison 501KB5 (4MW class, 34lbs/sec) Gas Turbine a summary of the benefits and associated cost are listed below. The cost of operation assumes that the effective cost for cyanuric acid is $0.27/lb and that 10-20% fuel consumption penalty (with/without heat recovery unit). (Note that if the system is a combined cycle system with a use for the additional heat generated this would not be considered an additional cost.)

Successful application of the RAPRENOX process to a gas turbine would offer the following advantages:

- Reduction of approximately 90% of the NO_x in a typical exhaust system with affecting gas turbine operation. We should be able to reach 18 ppm starting at 180 ppm.
- Retrofitable with exhaust, but not turbine modification, to allow for a reaction vessel installation.
- Reduction in CO and hydrocarbon concentrations possible due to inclusion of reaction vessel that makes secondary combustion part of the design.
- No slippage of ammonia or isocyanic acid observed.

- Is a cost effective means for reducing NOx without the addition of a hazardous chemical, such as ammonia, or the major cost of a large SCR catalyst installation.

The cost estimates for the operation of the RAPRENOX system on a 4MW gas turbine is derived from the following.

o Assumptions:

- 4MW gas turbine using 380 gallons fuel/hr.
- 27 lbs/hr NOx measured as NO2/hr
- 90% NOx removal efficiency
- $0.70/gallon for jet fuel

o Cost Calculations

- Using optimized system and assuming 1.9 lbs of cyanuric acid needed per pound of NOx for maximum NOx reduction
- Capital cost is approximated by cost of existing delivery system and appropriate reactor.

Table IV: Estimate of Cost for Application of RAPRENOX to Gas Turbine Exhaust

Estimate	High	Low
Installed Cost ($35/kW)	$140,000	$140,000
Annual Operating Cost @ 50% Annual Load Factor:		
Reagent Cost @ $0.27/lb and 1.9lbs/lb		$ 60,667
Reagent Cost @ $0.35/lb and 2.5lbs/lb	$103,500	
Additional Fuel @ 20% of fuel input and $0.70/gal.	$233,000	
Additional Fuel @ 10% of fuel input and $0.70/gal.		$118,000
	$ 4,000	$ 4,000
Other Operating and Maintenance @ 3% FCI		
Capital Charges @ 20%	$ 28,000	$ 28,000
Annual Total	$368,500	$210,667

In conclusion, the use of the RAPRENOX process for NOx control provides a cost effective method for reducing NOx emissions from gas turbines. The cost per pound of NO_x removed is between $1.78-$3.12. The use of the technology for gas turbines that employ a heat recovery would significantly reduce the operating cost of the technology and make it a clear choice for retrofit applications. It can also be used in other applications where the ability to follow load or provide NO_x reduction without the use of toxic ammonia is required.

7.0 FUTURE WORK:

Work is continuing on demonstrating this technology on an Allison 501 gas turbine. Long term testing and efforts to minimize nitrous oxide are being undertaken. In addition, interest from the gas turbine industry should provide

the needed support for applying this technology for NO_x reduction in gas turbines.

8.0 REFERENCES:

1. Elsener, M. and Koebel, M., "Analyse von Isocyansaeure, Blausaeure, Ammoniak und Lachgas in den Abgasen von Entstickungsprozessen", [Analysis of HNCO, HCN, NH_3 and N_2O in Effluents from NO_x Reduction Processes], Paul Scherrer Institut (Verbrennungstechnik), Reg. No. TM-51-89-21, Jul. 1989

2. Nicol, D., Malte, P.C., Lai, J., Marinov, N.N., Pratt, D.T., and Corr, R.A., " NO_x Sensitivities for Gas Turbine Operated on Lean – Premixed and Conventional Diffusion Flames", ASME Paper 92-GT-115, 1992

3. Correa, S.M., "A Review of NO_x Formation Under Gas–Turbine Combustion Conditions", Comb. Sci. and Tech. 87, pp. 329-362, 1992

4. Kee, R.J., Rupley, F.M. and Miller, J.A., "CHEMKIN-II: A Fortran Chemical Kinetic Package for Gas Phase Chemical Kinetics", Sandia National Laboratories Report SAND 89-8009, 1989

5. Kee, R.J., Rupley, F.M. and Miller, J.A., "The Chemkin Thermodynamic Data Base", Sandia National Laboratories Report SAND 87-8215 UC-4, 1991

6. Westbrook, C.K. and Pitz, W.J. "A Comprehensive Chemical Kinetic Reaction Mechanism for Oxidation and Pyrolysis of Propane and Propene" Combustion, Science and Technology, Vol. 37, 1984

7. Miller, J.A., and Perry, R.A., "An Exploratory Investigation of the Use of Alkali Metals in Nitrous Oxide Control" Int. Journal of Chemical Kinetics Vol. 28, 1996

8. Perry, R.A., "Application of RAPRENO$_x$ to Diesel Emission Control" Technology assessment and Research program for Offshore Minerals Operations, U.S. Department of the Interior Minerals Management Service, DOI No. 85K-SC293V, pp 185-190, 1991